

공학석사 학위논문

멀티빔에코사운더 개발을 위한 수치 시뮬레이션

Simulation Method for the Development of Multi-Beam Echo
Sounder

지도교수 김재수

2014년 12월

한국해양대학교

해양공학과

경효연

本 論文을 耿孝然의 工學碩士 學位論文으로 認准함.

위원장 공학박사 서 영 교 (인)

위 원 공학박사 김 기 만 (인)

위 원 공학박사 김 재 수 (인)



2014년 12월

한국해양대학교 대학원

해양공학과

경효연

Contents

Contents	i
List of Figures	iii
Abstract	v
1. Introduction	1
1.1 Background	1
1.2 Component of This Thesis	4
2. The System Composition and Theoretical Foundation	5
2.1 System Composition	7
2.1.1 Conversion	7
2.1.2 Signal Projection and Reception	8
2.1.3 Application of MBES System	8
2.2 Acoustic Principle of MBES	10
2.2.1 Sonar Equation	10
2.2.2 Beamforming	11
2.2.3 Beam Steering	15
2.3 The Operational Principle of MBES	19
2.3.1 Operational Principle	19
2.3.2 Mainly Measurement Error and Solution	22
3. The Design and Performance Analysis	24
3.1 Signal Selection	24
3.2 Backscattering Data Processing	26
3.1.1 Grazing Angle correction	26
3.1.2 Lambert's Law	28
3.3 Simulation and Results	30
4. Conclusions	32



< List of figures >

Fig. 1.1.1 Seafloor mapping.....	3
Fig. 2.1.1 Hardware of MBES.....	7
Fig. 2.1.2 Piezoelectric ceramics conversion principle.....	7
Fig. 2.2.1 Pencil beam response.....	12
Fig. 2.2.2 Directions of constructive and destructive interference for two projections with spacing $\lambda/2$	13
Fig. 2.2.3 Beam pattern of a multiple-element line array.....	14
Fig. 2.2.4 (a) Transmit and (b) receive beamformer.....	15
Fig. 2.2.5 Receive processing including variable delay.....	16
Fig. 2.2.6 Wavefront striking a hydrophone array from a source at angle θ	17
Fig. 2.2.7 Main lobe shifted to angle θ by introducing a time delay	17
Fig. 2.3.1 Projector array ensonifying a strip of the ocean floor	17
Fig. 2.3.2 Projector and hydrophone arrays arranged in <i>Mills Cross</i>	20
Fig. 2.3.3 Seabed backscatter bathymetric model.....	21
Fig. 2.3.4 Rotations about the ship center can eliminate these error	23
Fig. 3.2.1 Geometric configuration of incident angle.....	26
Fig. 3.2.2 Geometric configuration showing seabed slope effect.....	27
Fig. 3.2.3 Lambert's law for a scattering surface.....	29
Fig. 3.3.1 Two kinds of seafloor.....	30
Fig. 3.2.2 Continuous wave with center frequency 200 kHz.....	31
Fig. 3.3.3 LFM signal with center frequency 200 kHz.....	32
Fig. 3.3.4 Geometry of transmitter and receiver.....	32
Fig. 3.3.5 Received signal (with 2 times transmission loss) of each element of array (flat seabed).....	33
Fig. 3.3.6 Time-angle plot of a flat seabed.....	34

Fig. 3.3.7 Depth-acrosstrack plot of a flat seabed..... 34

Fig. 3.3.8 Received signal (with 2 times transmission loss) of each
element of array (flat seabed)..... 35

Fig. 3.3.9 Time-angle plot of a undulating seabed..... 35

Fig. 3.3.10 Depth-acrosstrack plot of a undulating seabed..... 36



Simulation Method for the Development of Multi-Beam Echo Sounder

by

Xiao Ran Geng

Department of Ocean Engineering
Graduate School of Korea Maritime University

ABSTRACT

Seafloor mapping using acoustic remote sensing technique is an attractive approach due to its high coverage capabilities and limited costs. The Multi-Beam Echo-Sounder (MBES) system provides high-resolution bathymetry and backscatter information with relatively perfect coverage. This paper described how the MBES system works and with the objective to get simulation images of it. The main theory of this thesis is sonar equation. The backscatter target strength is what we really needed. We present a simulation of seafloor mapping through backscatter data per beam, and because its performance is sensitive to seafloor type variation along the MBES swath so corrections for the angular dependence are applied. This simulation can support a wide range of survey applications including: hydrography, search and locate,

route survey and seafloor characterization. Also, a further discussion such as the doppler effect and sound speed correction should be discussed in the future.

Keywords: Multi-beam Echo-Sounder, Seafloor mapping, Back-scattering data, Lambert's law, Beam-forming.







Chapter 1 Introduction

1.1 Background

During the past decade, a model of the Multi-Beam Echo-Sounding process was developed. This technique provide an efficient way of sampling the mid-water column. These have been used extensively in fisheries and seafloor mapping.

Echo-sounding is a common technique to see underwater by acoustic means [1]. Different types of sonar systems are typically used for different purposes. Single beam echo-sounders are used in fisheries applications, to establish fish abundance estimates; hydro-graphic multi-beam sonars are used for seabed mapping; side-scan sonar is often used in studying the seabed habitat, sometimes in combination with data from single beam systems. Multi-beam systems collecting data for the full water column have the potential of being valuable in all these different fields at once.

Conventional survey systems used in seafloor mapping utilize either single beam, dual beam, or split beam techniques. A single beam system is not able to resolve individual targets. Although a dual beams or a split beam system can resolve individual targets, their performance and applicability are greatly degraded if multiple targets are present in the acoustic sample volume [2].

Multi-beam sonars can overcome these difficulties and have been

applied to target detection, tracking, and characterization in mid-water acoustic surveys. Compared to a single beam or split beam system, a multi-beam acoustic system is able to provide much larger volume coverage while maintaining a required spatial resolution. In addition, it can resolve multiple targets located at the same range simultaneously when the targets are separated larger than the angular resolution of the multi-beam sonar [3].

The field of seafloor mapping has diversified into many directions since the birth of the multi-beam echo-sounder in the 1960' s. At that time most of the development was related to the mechanical and electronic system components, whereas present research focuses on widely different areas, such as more precise bottom detection algorithms, seabed classification, image processing, acoustical modelling of the back-scattering process, and high resolution methods for direction finding of plane waves [4]. Multi-Beam Echo-Sounding thus encompasses many scientific disciplines.

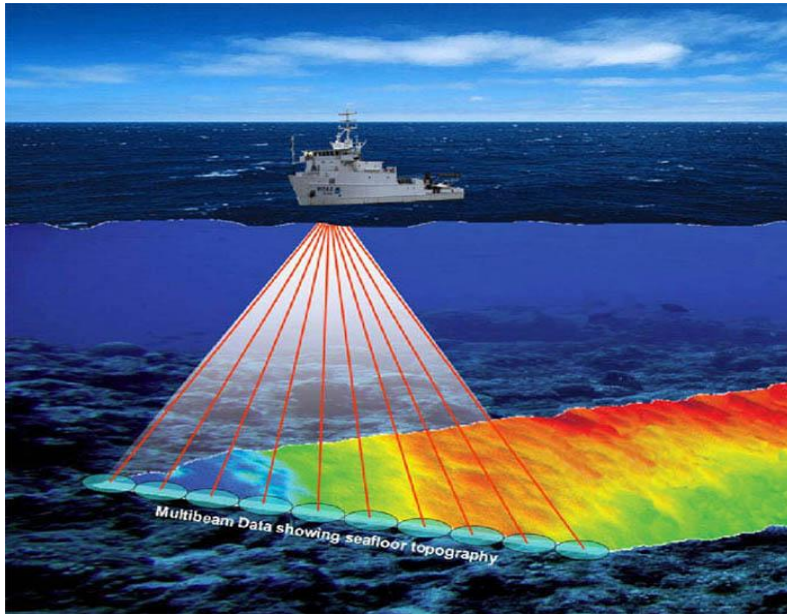
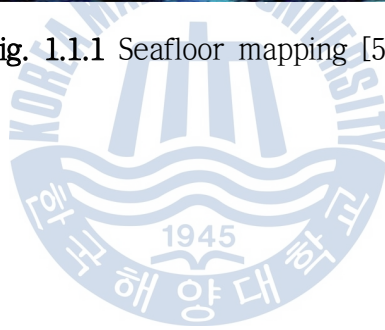


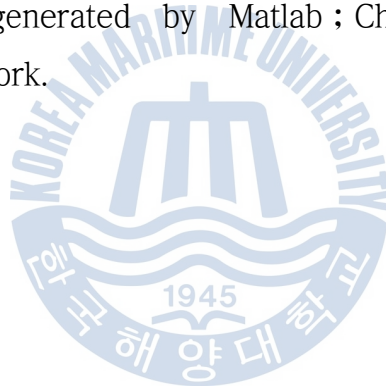
Fig. 1.1.1 Seafloor mapping [5]



1.2 Component of This Thesis

This thesis is based on the theory of Multi-beam Echo-Sounder, doing some research and investigation of it through rebuilding the key technology with the help of Matlab. The contents of the thesis are illustrated as follows:

Chapter 1 briefly introduces the background, motivation and outline of this work ; Chapter 2 describes the composition and elementary underwater acoustic theory of MBES. This chapter also introduces the operational theory of MBES ; Chapter 3 displays the simulated results generated by Matlab ; Chapter 4 gives the conclusion of this work.



Chapter 2 Theoretical Foundation of Multi-beam Echo-sounder

The Multi-Beam Echo-Sounder system conducts seafloor mapping in a stripe and relatively good coverage method by utilizing multiple transmit and multiple receiving. This technology is becoming more and more mature since it was introduced, which mostly depends on the rapid development of electronic technology, computer technology and material technology in recent years. Compared with the traditional single-beam echo-sounder, the MBES system has some advantages as follows:

1. high coverage for seafloor mapping;
2. high efficiency;
3. intensive data points;

With these advantages, MBES is replacing single-beam echo-sounder and has extensive applications in ocean survey. This chapter will talk about the technical principle of MBES.

2.1 System Composition

Multi-Beam Echo-Sounder is a united equipment system utilized for seafloor mapping or bathymetry. A ping will be generated by transducers beneath a ship's hull to produce a fan-shaped coverage of the seafloor. These systems measure and record the time for the acoustic signal to travel from the transmitter (transducer) to the seafloor (or object) and back to the receiver.

A holonomic MBES system should be composed of underwater transducers, deck equipments(computer, e.g) and post processing system(such as software like Matlab).

Figure 2.1.1 shows that a multi-beam system is a complex system consisted of several sub-systems. Although different multi-beam systems may varies on the number or composition of each elements, in general, we can consider multi-beam system as a combination of acoustic system, data collection system, data analysis system.

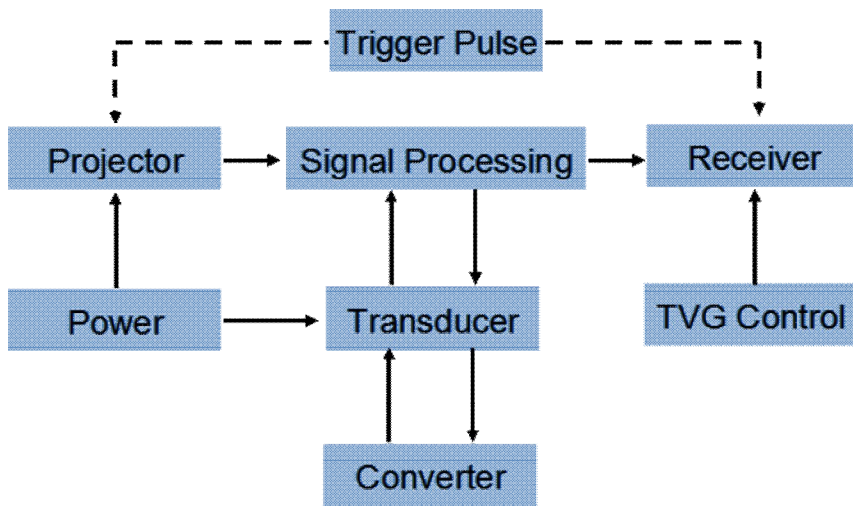


Fig. 2.1.1 Hardware of MBES

2.1.1 Conversion

The converter including projection array and receiving array. Different from single-beam survey, MBES system can generate several beams at the same time. Every element of converters is composed by piezoelectric ceramics, they work according to the piezoelectric effect, see Fig 2.1.2.

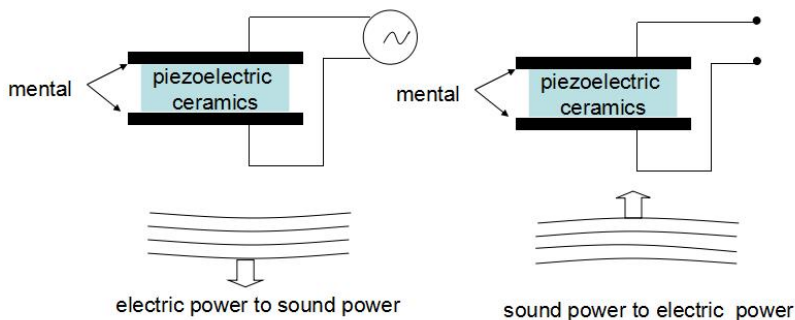


Fig. 2.1.2 Piezoelectric ceramics conversion principle [6]

When the converters are working, the projected beams in along-track usually are very narrow (3° in general), while much wider in across-track (140° usually).

2.1.2 Signal projection and Reception

During working time, the beams generated by MBES system forms a coverage strip on the seafloor, usually the width of the strip is determined by the launching angle while the launching angle was determined by system parameters.

Signal reception also relies on piezoelectric effect. During the process of receiving, the most obvious difference between single-beam system and MBES system is beam-forming and control system. When the acoustic wave is traveling, if it was not a vertical incidence, the travel path will be changed by effect of sound speed. The function of beam-forming and control system is to correct the travel path.

Also, sometimes TVG (Time-Varying Gain) is applied to compensate the transmission loss in the water, to make the back-scattering independent on the range or time.

2.1.3 Application of MBES System

The MBES system has quite outstanding advantages that other bathymetric system can't compare with, that's why it is widely used in ocean survey. This system can be used in fish schools detection, taking images of sediments both ocean and river floor, also searching about wrecks of missing craft.

And when we conduct a survey, the following factors should be considered:

1. Size and shape of the detected area;
2. water depth;
3. sea conditions;

because factor 1 affects the accuracy of received signal, according to Lamber's Law (See Chapter 3); factor 2 affects the strength of the projected and received signal which force us to change the center frequency of the signal; factor 3 mainly affects the physical error when receiving (See section 2.3.2).



2.2 Acoustic Principle of Multi-beam Echo-Sounder

2.2.1 Sonar Equation

The sonar equation is a systematic way of estimating the expected signal-to-noise ratios for sonar systems. It takes the source level, sound spreading, sound absorption, reflection losses, ambient noise, and receiver characteristics into account. The sonar equation is used to estimate the expected signal-to-noise ratios for all types of sonar systems. Slightly different versions of the sonar equation are used for active and passive sonar systems. In this thesis, we mainly talk about active sonar, which is also called echo-ranging sonar.

Active sonar systems, such as echosounders and side-scan sonars, transmit a pulse of sound and then listen for echoes. In an active sonar system the source also acts as a receiver.

The sonar equation usually written as:

$$SNR(\text{decibels}) = SL - 2TL + TS - NL \quad (2.1)$$

Parameters determined by the equipment:

Projector Source level: SL ;

Transmission loss: TL ;

Target strength: TS ;

Self-noise level: NL .

The echo level, EL , of the signal backscattered from the

bottom, may be derived from the sonar equation:

$$EL = SL - 2TL + BTS \quad (2.2)$$

Here, BTS is the bottom target strength, which is the back-scattering, in this thesis. The transmission loss consists of two parts, one due to spherical spreading of the signal, the other due to absorption loss in the water:

$$2TL = 2\alpha R + 40\log R \quad (2.3)$$

Here R is the range and α the absorption coefficient in dB/m. The bottom target strength will depend both on the reflective property of the seabed and the extent of the bottom which contributes to the back-scattering signal.

2.2.2 Beamforming

Beam-forming is a general signal processing technique used to control the direction of the reception or transmission of a signal on a transducer array [7]. Also beam-forming is a spatial filter, a means of transmitting or receiving sound preferentially directions over others [6].

The term beam-forming derives from the fact that early spatial filters were designed to form pencil beams (see polar plot in Fig.2.2.1) in order to receive a signal radiating from a specific location and attenuate signals from other locations [8].

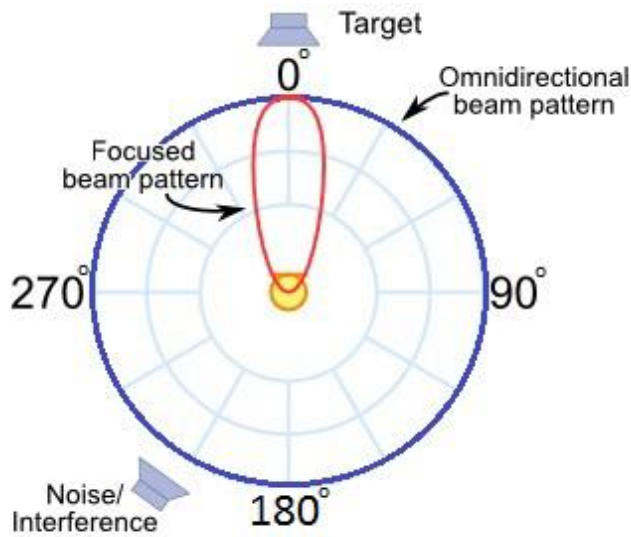


Fig. 2.2.1 Pencil beam response [9]

According to a former research [10], we can declare that the two projector arrays will transmit the highest energy sound in the directions $\theta = 0^\circ$, 180° , and no sound at all in the directions $\theta = 90^\circ$, 270° (See Figure 2.2.2). A typical sonar spacing d is $\lambda/2$, half a wavelength, because the angles at which destructive and constructive interference occur are most advantageous [11].

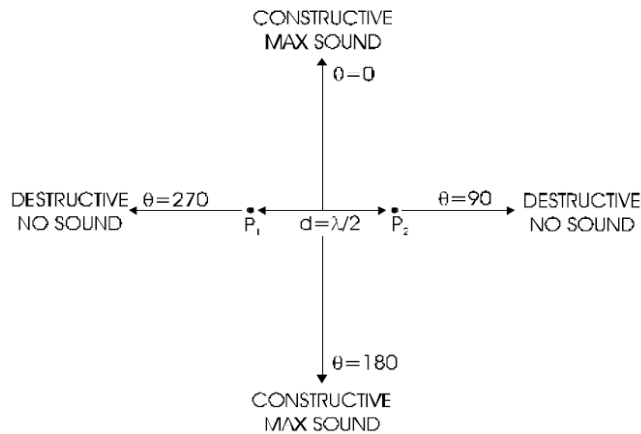


Fig. 2.2.2 Directions of constructive and destructive interference for two projectors with Spacing $\lambda/2$ [11]

Real projector arrays generally have more than two projector elements and have complex beam patterns. The beam pattern of a multiple-element line array is pictured in Figure 2.2.3. Through this figure we can see that on either side of the main lobe there is a series of side lobes takes place. The side lobes are an annoyance, not only is some of the projector energy being squandered in these directions, but there might be echoes from them as well, and these may be confused with the echoes from the target in the main lobe. Side lobes are unavoidable, but by using amplitude shading or weighting, it is possible to reduce the side lobes [11].

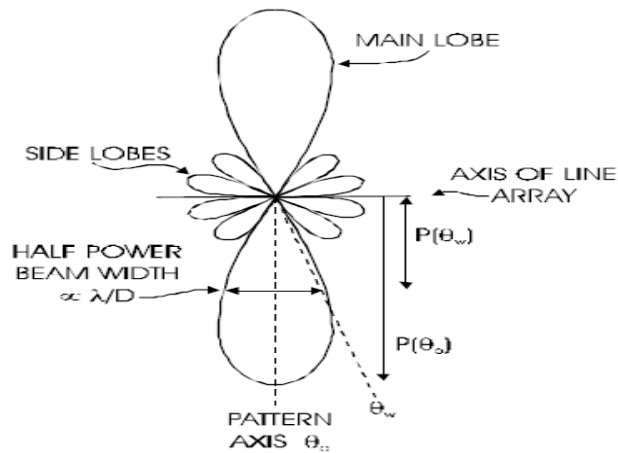
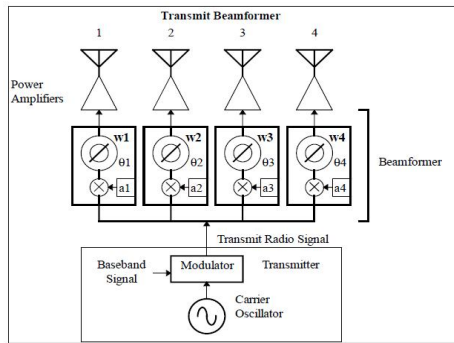


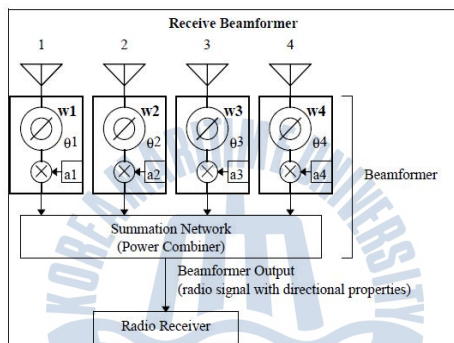
Fig. 2.2.3 Beam pattern of a multiple-element line array [11]

In beam-forming, both the amplitude and phase of each array element are controlled [12]. Combined amplitude and phase control can be used to adjust side lobe levels and steer nulls better than can be achieved by phase control alone. The combined relative amplitude a_k and phase shift θ_k for each antenna is called a *complex weight* and is represented by a complex constant w_k , where k for the k^{th} antenna.

A beamformer for a radio transmitter applies the complex weight to the transmit signal (shifts the phase and sets the amplitude) for each element of the array array. A beamformer for radio reception applies the complex weight to the signal from each array element, then sums all of the signals into one that has the desired directional pattern. See Figure 2.2.4.



(a)



(b)

Fig. 2.2.4 (a) Transmit and (b) receive beamformer [10]

2.2.3 Beam Steering

How an array can be altered to receive preferentially from any of a number of directions is called beam steering [11].

The receive processing for a phase array scanner required for both steering and dynamic focusing is illustrated in Figure 2.2.5.

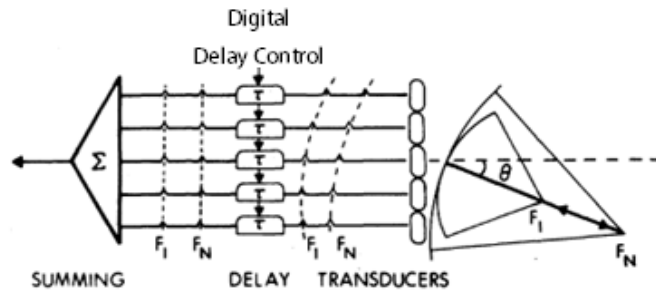


Fig. 2.2.5 Receive processing including variable delay [12]

Consider a line array receiving sound from an arbitrary angle θ off the perpendicular (Figure 2.2.6). As the sound waves must travel different distances to reach each hydrophone, causing the signals at the different hydrophones to add destructively. In Figure 2.2.6, the distance between each element of array is d , sound waves first strike the hydrophone labeled 3. They must travel the distance labeled A before reaching hydrophone 2, and distance B before reaching hydrophone 1. These distances can be computed using the spacing between the hydrophones:

$$\begin{aligned} A &= d \times \sin \theta \\ B &= 2d \times \sin \theta \end{aligned} \quad (2.4)$$

The extra times required for the wave front to reach each hydrophone are given by the distances divided by the local sound speed c :

$$\begin{aligned} T_2(\text{time to hydrophone 2}) &= A/c = (d \sin \theta)/c \\ T_1(\text{time to hydrophone 1}) &= B/c = (2d \sin \theta)/c \end{aligned} \quad (2.5)$$

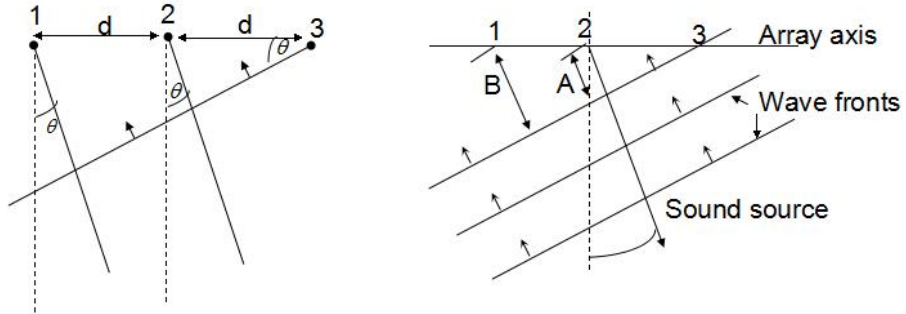


Fig. 2.2.6 Wavefronts striking a hydrophone array from a source at angle θ

In this example, we would sum the reading of hydrophone 3 with the reading of hydrophone 2 delayed by T_2 and the reading of hydrophone 1 delayed by time T_1 . This is called *time delay*. It causes the main lobe of the beam pattern to shift such that its axis is at angle θ from the perpendicular (see Figure 2.2.7). By applying time delays and summing them, an array can be “steered” to maximize its sensitivity to any angle θ .

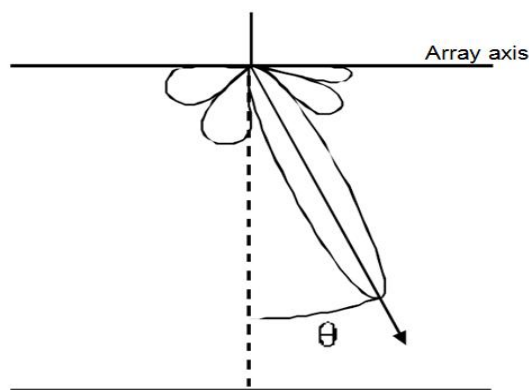


Fig. 2.2.7 Main lobe shifted to angle θ by introducing a time delay

Note that in steering a hydrophone array to be sensitive to a particular angle, nothing about the array itself is changed, only the interpretation of the data it records is altered. By changing the data processing, the same array can be steered to observe any of a large range of angles. In fact, using the same recorded data from the elements of the hydrophone array, different data processing can be used to examine the sounds coming from different angles simultaneously. In this way, a hydrophone array can be used to examine the echoes from a single ping at many different locations.



2.3 The Operational Principle of MBES

2.3.1 Operational Principle

Multi-beam echo sounders, like other sonar systems, emit sound waves in the shape of a fan from directly beneath a ship's hull. These systems measure and record the time it takes for the acoustic signal to travel from the transducer to the seafloor and back to the receiver. In this way, multi-beam sonars produce a “swath” of soundings for broad coverage of a survey area and the coverage area on the seafloor depends on the depth of the water.

Most modern systems work by transmitting a broad acoustic fan shaped pulse from a specially designed transducer across the full swath across track with a narrow along track then forming multiple receive beams that is much narrower in the across track.

In reality, A projector line array transmits sound preferentially in all directions perpendicular to the axis of the array, ensonifying a strip of the ocean bottom. See Figure 2.3.1.

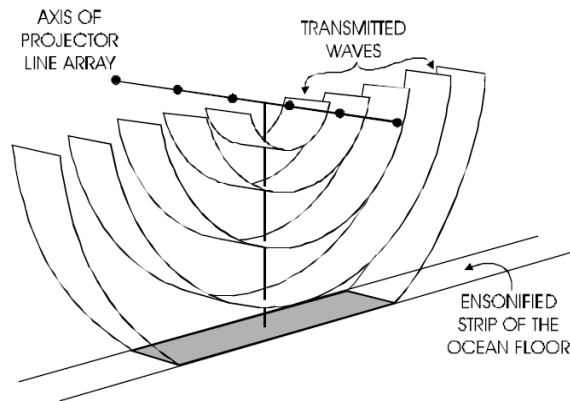


Fig. 2.3.1 Projector array ensonifying a strip of the ocean floor [11]

If the projector and hydrophone arrays are perpendicular to each other, the perpendicular arrangement of the projector and hydrophone line arrays is called a *Mills Cross*. In this situation, the strip of the ocean floor ensonified by the projectors will intersect with the strip of the ocean floor observed by the hydrophones.

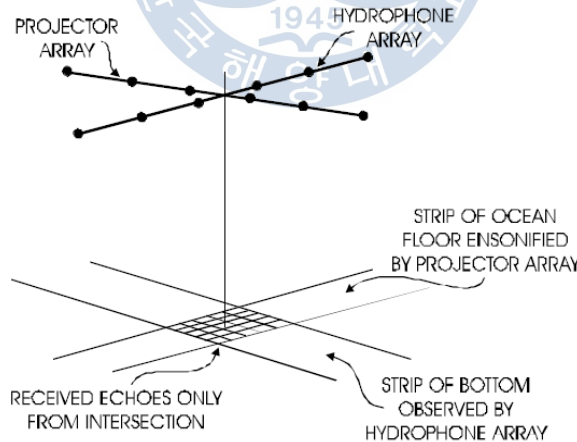


Fig. 2.3.2 Projector and hydrophone arrays arranged in *Mills Cross* [11].

When the transmit and receive beam patterns are multiplied together, the projected product, represents a series of semi-elliptical footprints lying primarily along the axes of the two main lobes. The strongest seabed echo should normally be received from the central mainlobe-mainlobe intersection. The illustrating of full transmit ensonification and receiver sensitivity pattern is displayed by Figure 2.3.3.

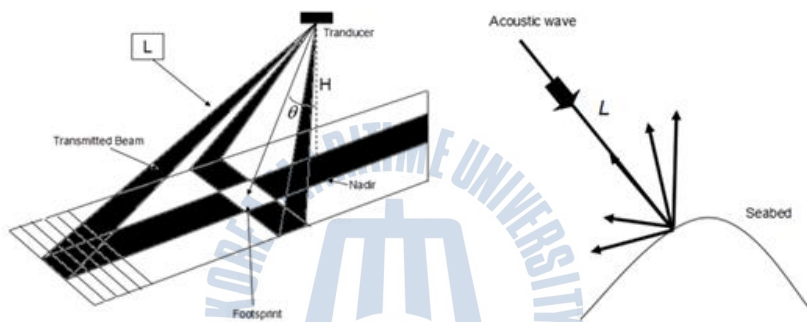


Fig. 2.3.3 Seabed backscatter bathymetric model

Supposing a transmitted beam ensonified into the seabed at a incident angle θ , the transmitted signal will scatter along every directions. Some of these scatters will be reflected by the seabed in the backward direction. See Figure 2.3.4.

If we can receive and measure the delayed time(Δt) of this backscatter, then the length L can be calculated. L is called *travel path*.

$$L = C \times \frac{\Delta t}{2} \quad (2.6)$$

In this expression, C is the sound speed, Δt is the time which a signal needs from generating to back receiving.

$$\begin{aligned} H &= L \times \cos\theta \\ RX &= L \times \sin\theta \end{aligned} \quad (2.7)$$

In this expression, H is the depth of a point which will be tested, RX is the corresponding horizontal position.

2.3.2 Mainly Measurement Error and Solution

In order to solve any complicate circumstances in underwater survey, plenty of advanced equipments were applied in multi-beam echo-sounder. So the deviations of each equipment is of great meaning for engineers. The mainly deviations usually including mounting error, movement error, sound speed error and near-field error.

(1) Mounting error: The equipments need mounted including transducer, GPS antenna and moving sensor. They mounted at different position in a vessel, when the vessel moves, all of them have different moving direction and amplitude, causing bathymetric error. By setting geometric reference points before mounting, measuring mounting angle and position corresponding to reference points carefully, we can make compensation for this error.

(2) Movement error: Coming from vessel sailing, turning, speed changing and bumping. It can be avoided by navigation software and movement sensor adjustment. Also it's a artifice to maintain the vessel under a steady speed.

(3) Sound speed error: The physical character varies as the depth of ocean increasing. Temperature and salinity will cause the changing of density, as a result, the acoustic wave travels in a curved path. That causes measurement error at every depth point. Because of this, we usually measure sound speed profile to calculate acoustic wave propagates path.

(4) Near-field error: If the reflection point is close to projection point, then reverberation arises. It is difficult to identify signal and noise. The operation staff can adjust parameters according to the environment and make compensation with the help of processing software.

Also, there are other circumstances to cause error, typically are pitch, roll and yaw(See figure 2.3.4) and a process called *motion compensation* can eliminate these error.

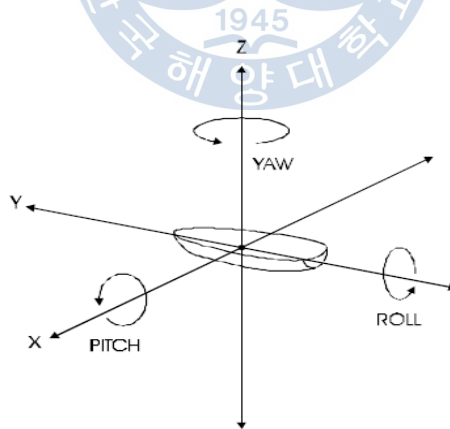


Fig. 2.3.4 Rotations about the ship center can eliminate these error [11].

Chapter 3 The Design and Performance Analysis

3.1 Signal Selection

There are two kinds of signals can be used in this paper: continuous wave pulse (CW pulse) and Linear Frequency Modulation (LFM pulse).

The CW pulse is an electromagnetic wave of constant amplitude and frequency, and in mathematical analysis, of infinite duration. Both advantages and disadvantages are notable for CW signal. First, the CW signal can be generated by very simple equipments. It is a very convenient type of signal because its frequency is fixed and the higher the frequency is, the better image resolution we can get. However, in the environment of ocean, high frequency signal can only travel in a very short distance, for detecting long range scale, that requires us using low frequency signals which provides contaminating data.

To solve the problems mentioned above, people introduced the linear frequency modulation. The LFM signal also known as Chirp signal. A "Chirp" is a signal in which the frequency

$$f(t) = f_0 + kt \quad (3.1)$$

increases or decreases with time. Here f_0 stands for frequency at $t = 0$, k means changing rate. It is also an ingenious way of handling a practical problem in echo location systems, such as radar and sonar because radar and sonar needs short time pulse but sustainable signal. Also, chirp signal is insensitive to

doppler-shift which means the moving of the vessel has little impact on the behavior of hydrophones



3.2 Backscattering Data Processing

3.2.1 Grazing Angle Correction

During each survey, the back-scattering data were collected over a common area of immobile seabed. The echo amplitudes as measured by the MBES are determined by back-scattering from the seafloor, a process dependent on the nature of the seafloor, i.e., its composition, orientation, roughness and geo-acoustic properties. In this paper, we discuss two kinds of seabed : flat seabed and undulating seabed in a *sine* shape. Also, we consider the environment as perfect, there is no ray bending, and the acoustic energy is redistributed into the upper medium, with none lost by transmission into the medium below.

We start from a easy situation that the seafloor is flat. Supposing a vessel is traveling along an arbitrary direction carrying a MBES system. According to Figure 3.2.1 we can calculate the incident angle ω of the transmitted beam.

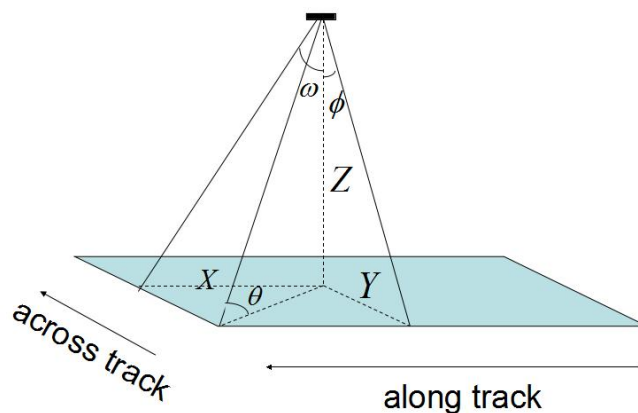


Fig 3.2.1 Geometric configuration of incident angle

$$\theta = \tan^{-1} \frac{1}{\sqrt{\tan^2 \omega + \tan^2 \phi}} \quad (3.2)$$

With

ω : incident angle of along track,

ϕ : incident angle of across track,

θ : real incident angle,

Under this situation, the bottom backscatter strength will decrease markedly at ranges away from normal incidence. However, more dynamic topography may present inward facing slopes, also, in the reality, there exists extreme geometries for example man-made structures or natural obstacles such as big rock or coral reefs. So the seabed won't be as flat as a mirror. According to Figure 3.2.2, we take slopes both along track and across track into consideration.

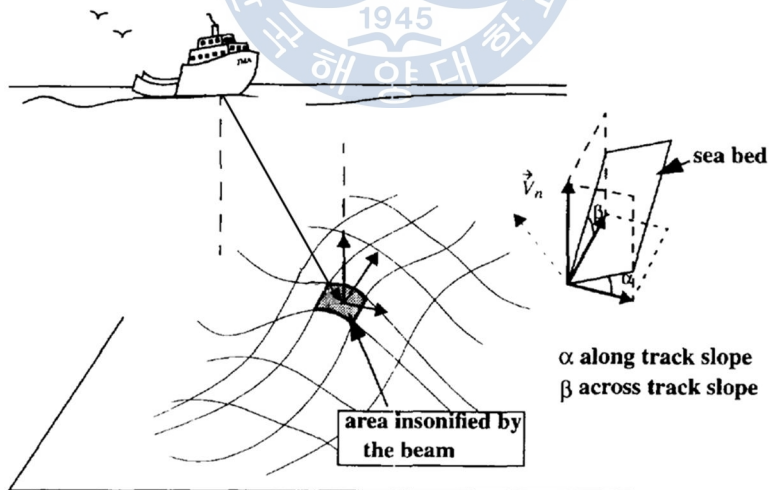


Fig 3.2.2 Geometric configuration showing seabed slope effects [12]

Solving the incident angle gives:

$$\theta_s = \arctan \frac{1}{\sqrt{\tan^2(\omega + \alpha) + \tan^2(\phi + \beta)}} \quad (3.3)$$

With the help of equation (3.2) and (3.3), we get the real incident angle of a transmitted beam both on a flat seabed and a undulating seabed.

3.2.2 Lambert's Law

To calculate scattering from the seafloor is the core of this paper. The function called Lambert's Law is a type of angular variation which many rough surfaces appear to satisfy for the scattering of both sound and light [14]. In Figure 3.2.3, we set sound intensity I_i be incident at angle θ on the small surface area dA . The power received by dA will be $I_i \sin \theta dA$. This power is assumed to be scattered proportionately to the sine of the angle of scattering, so that the intensity at unit direction ϕ will be [15]

$$I_i = \mu I_i \sin \theta \sin \phi dA \quad (3.4)$$

where μ is a proportionality constant. And in the backward direction, for which $\phi = \pi - \theta$ [15],

$$I_i = \mu I_i \sin^2 \theta dA \quad (3.5)$$

Thus, by Lambert's law, the backscattering strength must vary as the square of the sine of the grazing angle. This equation is a precisely description of the back-scattering of sound by very

rough bottoms.

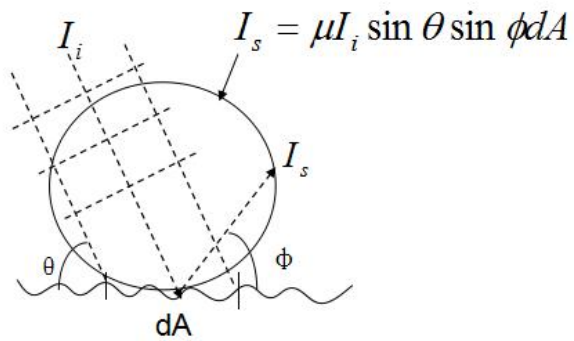


Fig. 3.2.3 Lambert's law for a scattering surface [15]



3.3 Simulation and Results

3.3.1 Simulation Description

In this section, the performance of the MBES is analyzed. The technical specifications of this system are as follows:

- (1) The depth of area under survey is 30m.
- (2) The maximum angular coverage is 90° ($-45^\circ \sim 45^\circ$).
- (3) The transducer geometry is mills cross.

The bathymetry of this study area is shown in Fig. 3.3.1, patches $0.5 \times 0.5 \text{ m}^2$, both flat seabed and a sinusoid fluctuation seabed were presented based on the methodology developed above. To assess the MBES classification results, a comparison is made with the analysis of the CW pulse and chirp pulse.

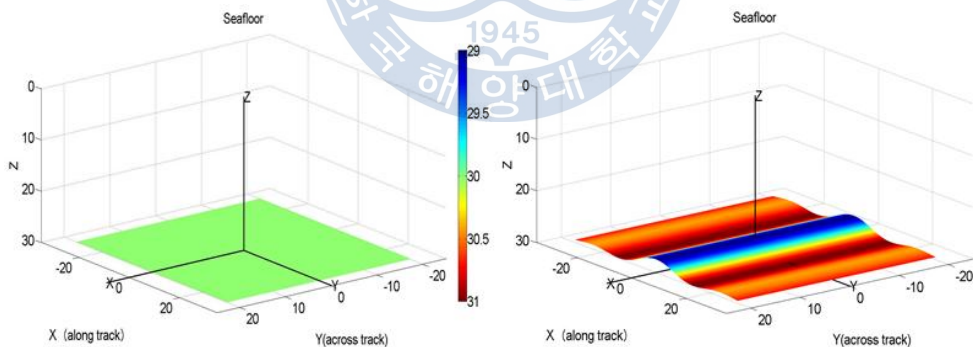


Fig. 3.3.1 Two kinds of seafloor. The left is flat seabed and the right is undulating seabed with a 2 meters high cardinal sine function

The geometry of projectors and hydrophones is shown in Fig 3.3.2. Both of them are 2 x 64 plane array and intersected with each other perpendicularly.

For the CW wave, the pulse length is $300\mu\text{s}$, center frequency is 200kHz, we choose frequency region between 190 kHz - 210 kHz, getting band-limited signal which is the CW pulse we will use in the following simulation. As for the chirp signal, the frequency interval is 130 kHz - 270 kHz. The information of two kinds of signals is shown in Fig 3.3.2 and Fig 3.3.3.

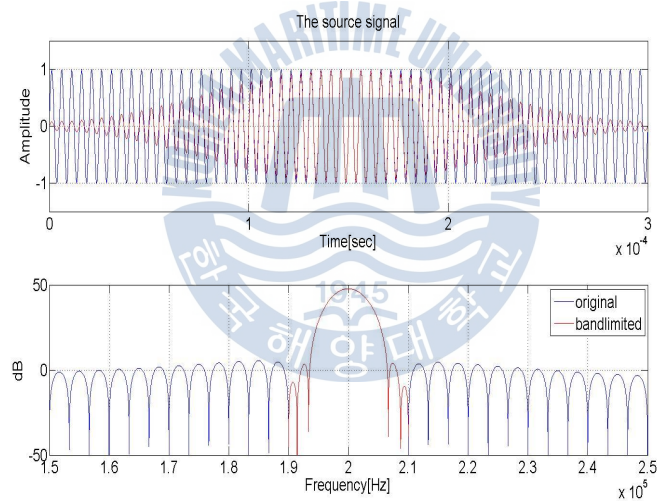


Fig. 3.3.2 Continuous wave with center frequency 200 kHz. The bottom is frequency spectrum and we choose 190kHz-200kHz to do simulation.

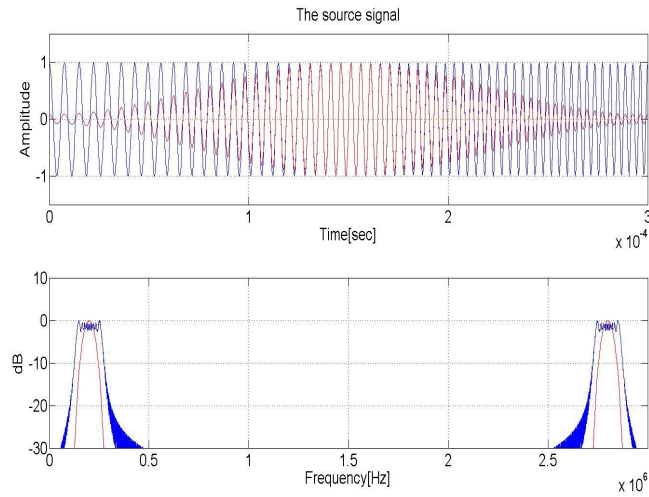


Fig. 3.3.3 LFM signal with center frequency 200 kHz. The bottom is frequency spectrum, the initial frequency is 130kHz and target frequency is 270kHz.

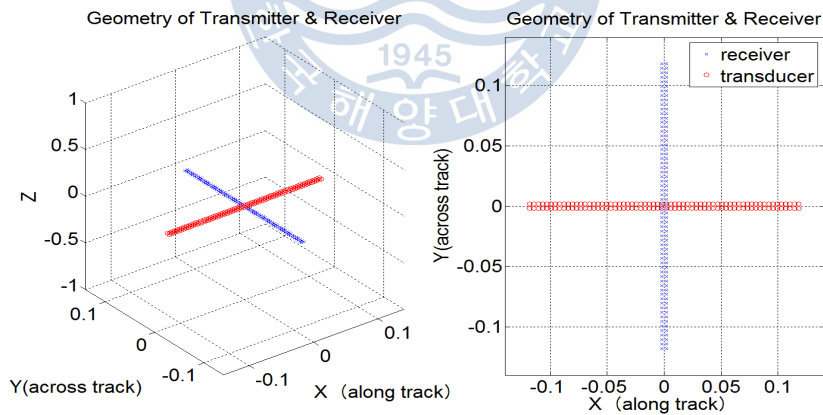


Fig. 3.3.4 Geometry of transmitter and receiver

3.3.2 Simulation Results

A. Flat Seabed

We start the simulation of seafloor with the flat seabed. The shape of the seafloor was shown as Fig 3.3.1 left. As we talked above, the simulation will be conducted with both CW pulse and LFM signal.

The received signal of each element of receivers, please see Fig 3.3.5. The seafloor mapping of a flat seabed is shown in Fig 3.3.6, which is a time-angle plot. This difference can be seen more clearly in a depth-acrosstrack plot (See Fig 3.3.7). In this picture we can see that the depth-acrosstrack figure presented to be more smooth under LFM signal.

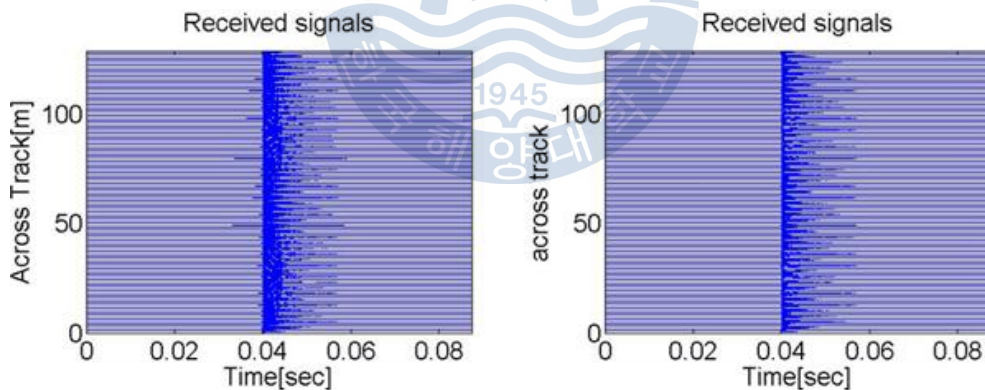


Fig. 3.3.5 Received signal (with 2 times transmission loss) of each element of array (flat seabed). The left is under continuous wave, and the right is under LFM signal.

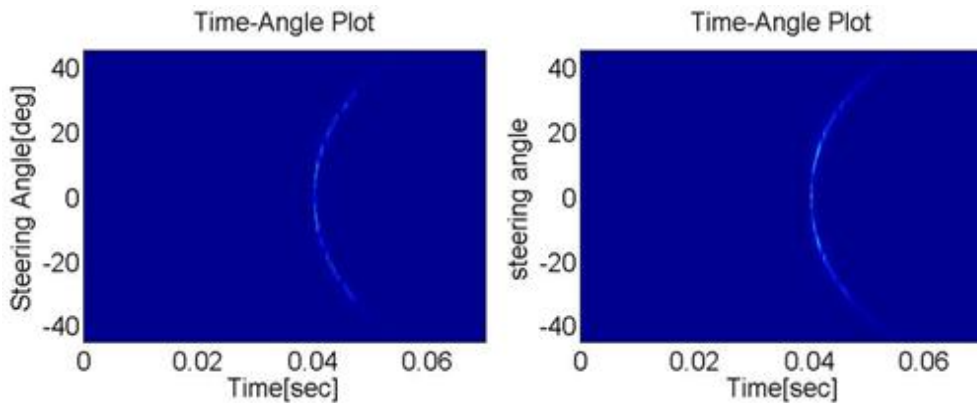


Fig 3.3.6 Time-angle plot of a flat seabed. Left is under CW pulse and right is under chirp signal

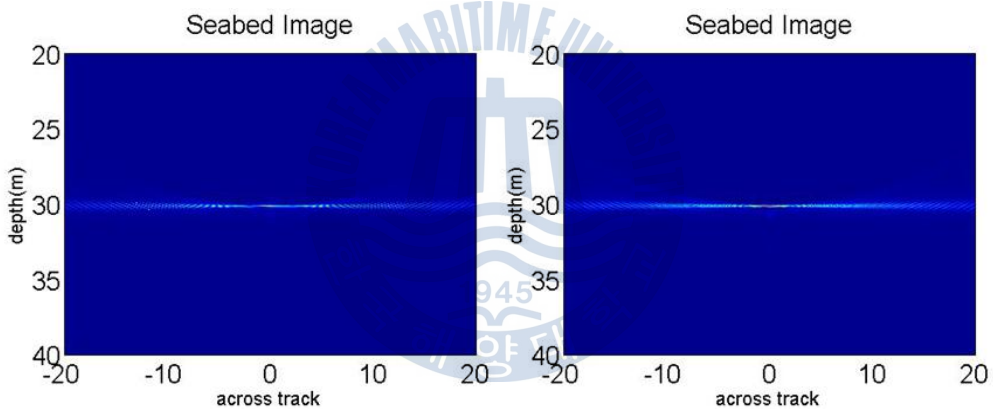


Fig 3.3.7 Depth-acrosstrack plot of a flat seabed. Left is under CW pulse and right is under chirp signal

B. Undulating Seabed

In the reality, the seabed won't be as flat as a mirror, so the undulating seabed has more realistic meanings in simulation. Also, the shape of the seabed has already been shown in Fig 3.3.1 right. It is a sinc-wave shape seabed, with the height about 2 meters.

Fig 3.3.8 is also the received signal for undulating seabed. As shown in Fig 3.3.9, the gently undulations of the seafloor can be seen clearly which matches the up-and-downs. Also, a depth-acrosstrack plot is shown in Fig 3.3.10, the advantages of LFM signal is still obviously.

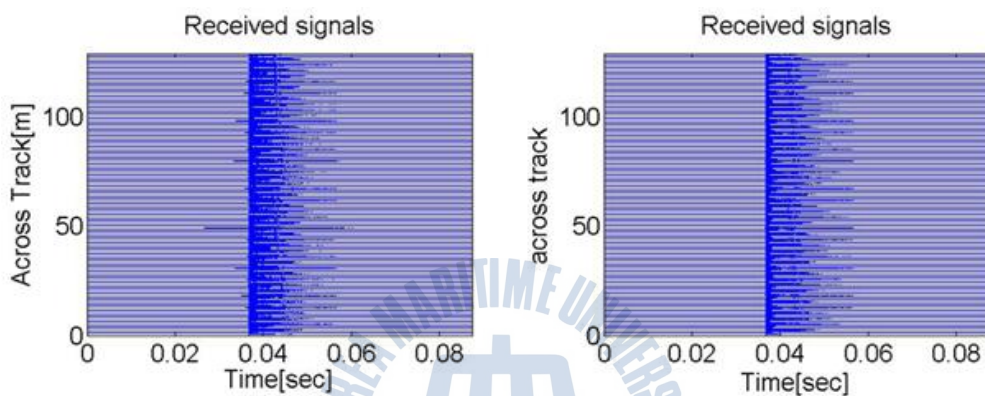


Fig. 3.3.8 Received signal (with 2 times transmission loss) of each element of array (undulating seabed). The left is under continuous wave, and the right is under chirp signal

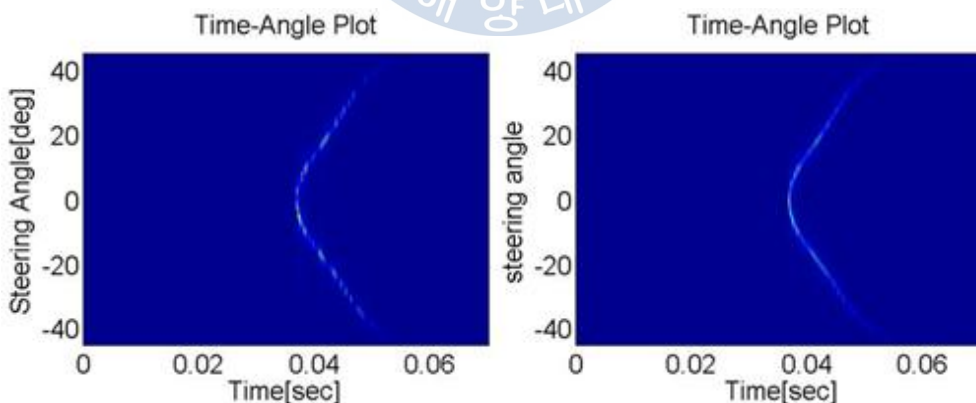


Fig 3.3.9 Time-angle plot of a undulating seabed. Left is under CW pulse and right is under chirp signal

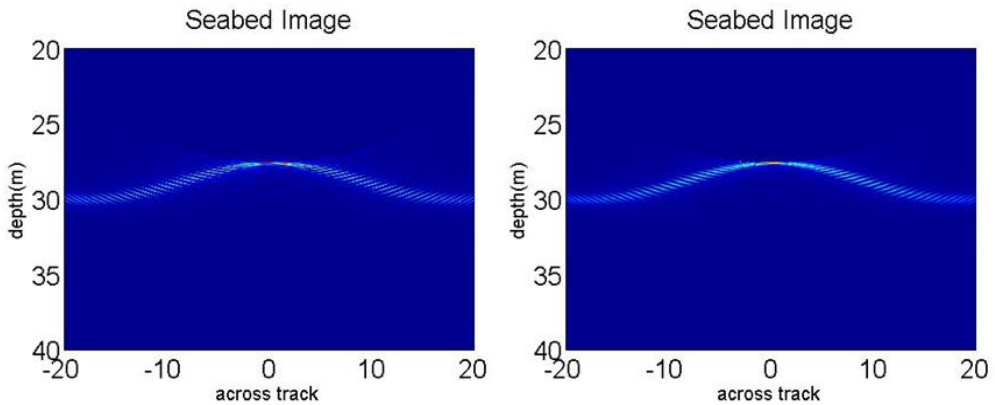
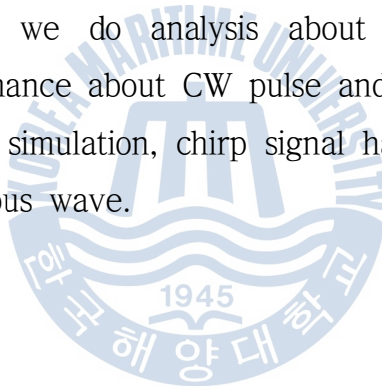


Fig 3.3.10 Depth-acrosstrack plot of a undulating seabed. Left is under CW pulse and right is under chirp signal

In this Chapter, we do analysis about the simulation. We examine the performance about CW pulse and chirp signal and we can see that in the simulation, chirp signal has no doubt a better results than continuous wave.



Chapter 4 Conclusion

Seabed mapping or bathymetry using MBES, back-scattering data is a promising approach.

In this thesis, a simulation for a certain area of seafloor was conducted. The theory foundation of MBES is beamforming, and the mills cross technique was also introduced briefly. In practise, to get accurate data, we have to deal with the errors and do some correction before and after the data acquisition.

As the seabed may be not flat, the degree to which different bottom types can be discriminated using the back-scattering data depends on the presence of local slopes of the seafloor. So we need Lamber's Law to do local slope correction.

This thesis presented a methodology to use high-frequency MBES data for the seafloor mapping and this simulation can support a wide range of survey applications including: hydrography, search and locate, route survey and seafloor characterization.

References

[1] B. Buelens¹, R. Williams¹, A. Sale¹, T. Pauly , "Model Inversion for Midwater Multibeam Backscatter Data Analysis," OCEANS 2005 - EUROPE, Vol. 1, pp. 431-435. 2005.

[2] Dezhang Chu, Kenneth C. Baldwin, Kenneth G. Foote, Yanchao Li, Larry A. Mayer, Gary D. Melvin , "Multibeam sonar calibration: removal of static surface reverberation by coherent echo subtraction," MTS/IEEE CONFERENCE AND EXHIBITION, Vol. 4, pp 2498-2502. 2001.

[3] Dezhang Chu, Lawrence C. Hufnagle, Jr. , "Time varying gain (TVG) measurements of a multibeam echo sounder for applications to quantitative acoustics," OCEANS 2006.

[4] Dezhang Chu, Kenneth C. Baldwin, Kenneth G. Foote, Yanchao Li, Larry A. Mayer, Gary D. Melvin , "Multibeam sonar calibration target localization in azimuth," OCEANS, 2001. MTS/IEEE Conference and Exhibition, Vol. 4, 2506 - 2510, 2001.

[5] <http://continentalshelf.gov/missions/10arctic/logs/aug07/.html>

[6] J.S.Ding, X.H.Zhou, Z.C.Liu, W.H.Zhang, "Working Theory of Multi-Beam Echo Sounder", China Academic Journal Electronic Publishing House, 1994-2008.

[7]An Introduction to Beamforming <http://staff.washington.edu/aganse/beamforming/beamforming.html>

[8] A.D.Waite, "Sonar for Practising Engineers, Third Edition," JOHN WILEY & SONS, LTD.

- [9] M. Aarts, H. Pries, A. Doff, "Two Sensor Array Beamforming Algorithm", Delft University of Technology, 2012
- [10] Toby Haynes, "A Primer on Digital Beamforming," Spectrum Signal Processing, 1998.
- [11] "Multi-beam Sonar Theory of Operation," L-3 Communications SeaBeam Instruments, 2000.
- [12] OLAF T. Von Ramm, S.W. Smith, "Beam Steering with Linear Arrays", IEEE Transactions on Biomedical Engineering, Vol. BME-30, No. 8, August 1983.
- [13] P. Vincent, C.Sintes, F. Maussang, X. Lurton, R. Garello, "Doppler Effect on Bathymetry using Frequency Modulated Multibeam Echo Sounders", Oceans, 2011 IEEE, p1-p5.
- [14] William S.Burdic, "Underwater Acoustic System Analysis," Prentice-Hall, Inc., Englewood Cliffs, New Jersey, 1984.
- [15] R. J. Urick, "Principles of underwater sound, 3d edition," McGraw-Hill Book company, 1983.

감사의 글

2011년 중국 대련해양대학교 졸업한후 한국해양대학교 대학원에 입학하고 나서 벌써 2년반이라는 시간이 흘렀습니다. 추억이 가득했던 지난 2년간의 대학원 생활을 돌아보며, 이글로써 감사의 인사를 드립니다. 부족한 저에게 논문을 쓸 수 있게 해준 모든 분들에게 이 자리를 빌어 감사의 마음을 전합니다.

먼저 저에게 지속적인 가르침과 많은 조언을 해주신 김재수 교수님께 마음 속여 감사를 드립니다. 항상 건강하시고 행복하시길기원합니다. 그리고 바쁘신 와중에서도 논문 심사를 해 주시고 격려를 해 주신 서영교 교수님과 김기만 교수님께 진심으로 감사드립니다. 항상 저를 아끼시며 관심을 주신 교수님들께 감사를 드립니다.

대학원생활을 즐겁게 할 수 있게 해준 수중음향연구실 동료들에게 깊은 감사를 드립니다. 같은 연구실에서 고생한 지성형,기훈형에게 미안함과 고마움을 함께 전합니다. 그리고 항상 옆에 도와주는 윤희누나, 민정누나, 정홍형, 상윤형, 세현형, 같은 공부하고 소중한 동현형, 남기, 동환, 성일, 용화에게도 감사합니다.

또한 우리 가족들에게 감사의 마음을 전합니다. 이 때까지 저를 잘 키워 주신 부모님, 그리고 2년간 피곤에 지치고 힘들 때마다 늘 곁에서 힘이 되어 주고 응원해준 모든 친구들에게 고마움과 사랑하는 마음을 전합니다.